Full-Polymer Cholesteric Composites for Transmission and Reflection Holographic Gratings

Alexander Ryabchun,* Oksana Sakhno, Joachim Stumpe, and Alexey Bobrovsky

A new type of self-organized materials based on cholesteric networks filled with photoactive side-chain copolymer is being developed. Supramolecular helical structure of cholesteric polymer network resulting in the selective reflection is used as a photonic scaffold. Photochromic azobenzene-containing nematic copolymer is embedded in cholesteric scaffold and utilized as a photoactive media for optical pattering. 1D and 2D transmission diffraction gratings are successfully recorded in composite films by holographic technique. For the first time the possibility to create selective reflection gratings in cholesteric material mimicking the natural optical properties of cholesteric mesophase is demonstrated. That enables the coexistence of two selective gratings, where one has an intrinsic cholesteric periodic helical structure and the other is a holographic grating generated in photochromic polymer. The full-polymer composites provide high light-induced optical anisotropy due to effective photo-orientation of side-chain fragments of the azobenzene-containing liquid crystalline polymer, and prevent the degradation of the helical superstructure maintaining all optical properties of cholesteric mesophase. The proposed class of optical materials could be easily applied to a broad range of polymeric materials with specific functionality. The versatility of the adjustment and material preprogramming combined with high optical performance makes these materials a highly promising candidate for modern optical and photonic applications.

1. Introduction

Today a great attention of science and industry is directed toward developing novel materials which can give useful optical feedback by the interaction with light. In this respect,

cholesteric liquid crystalline (LC) materials characterized by supramolecular helical architecture are drawing significant interest as stimuli-responsive functional smart materials.[1,2] Cholesteric liquid crystals can be regarded as 1D photonic structure exhibiting a relatively wide band gap. The center of the band and its width are determined by Equations (1) and (2), respectively

$$\lambda_{\max} = nP \tag{1}$$

$$\Delta\lambda_{\max} = \Delta nP \tag{2}$$

where n is the average refractive index, P is the cholesteric helix pitch, and Δn is birefringence. The tuning of the photonic bad gap can be achieved by control of the supramolecular cholesteric pitch which might be sensitive to temperature, electric field, light, and other stimuli, whereas the bandwidth is affected by the gradient of the helix pitch or by changes in refractive indices.[3–5]

The common method to induce cholesteric mesophase is doping nematic LCs with chiral molecules transducing their molecular chirality to supramolecular level. It is known that if the nematic hosts are doped with so-called photoactive chiral switches or molecular motors, cholesteric helical structure and consequently optical properties can be effectively and reversibly varied by light irradiation.[6–9]

In order to obtain cholesteric structure in the form of solid or soft materials mesogenic molecules can be covalently attached to polymer networks so that the supramolecular structure is being imprinted.[10–18] The introduction of different functional fragments into the cholesteric network allows films, coatings, fibers, drops, etc. to change their optical properties under various external stimuli. The crosslinked polymer structure provides stability, good mechanical properties and reversibility of the structural changes of such responsive materials. In a number of works the concept of exploiting of cholesteric networks as templates or supports for variety of low-molar-mass as well as polymeric materials is demonstrated.[19–23] Various optical sensors based on functionalized cholesteric polymers networks were also reported.[24–26] Previously we applied this concept for the introduction of low-molar-mass nematic mixture capable to undergo light-induced phase transition into the cholesteric scaffolds in order to develop materials with tunable optical properties.[27]

Dr. A. Ryabchun
Bio-Inspired and Smart Materials
MESA+ Institute for Nanotechnology
University of Twente
PO Box 207, 7500 AE Enschede, The Netherlands
E-mail: ryabchunmsu@gmail.com, a.ryabchun@utwente.nl

Dr. A. Ryabchun, Dr. O. Sakhno
Fraunhofer Institute for Applied Polymer Research
Geiselbergstr. 69, 14476 Potsdam-Golm, Germany

Dr. J. Stumpe
Chemistry Department
University of Potsdam
Am Mühlenberg 11, 14476 Potsdam, Germany

Prof. A. Bobrovsky
Faculty of Chemistry
Moscow State University
Lenin Hills, 119991 Moscow, Russia

**ADVANCED
SCIENCE NEWS**
www.advancedsciencenews.com

**ADVANCED
OPTICAL
MATERIALS**
www.advopticalmat.de

Another uncommon way of exploiting cholesteric LC materials is the creation of controllable optical elements, particularly, diffraction gratings.[28–32] One of the approaches is the optical structuring of cholesteric side-chain polymers containing azobenzene fragments by means of UV or visible holography.[28,30,33–35] This method makes use of the unique combination of high optical anisotropy inhering in LC state with the possibility of the effective light-induced control of optical properties due to E–Z photoisomerization of azobenzene molecules. Such LC materials can be applied for the optical information recording and for data storage,[36–41] optoelectronics, and photonics.[42–44]

In a number of studies it was shown that the optical recording of polarization (orientational) or surface relief gratings (SRGs) in cholesteric materials results in gradual degradation of supramolecular helical structure and, consequently, in the loss of unique optical properties of the cholesteric phase.[28,33] However, in our previous work we have demonstrated the partial preserving of cholesteric helix by adjusting the conditions of holographic structuring providing a so-called "double" information recording.[30] It was shown that such diffraction gratings possess moderate efficiency and stability.

In the current contribution, in order to overcome the degradation of the supramolecular helical structure during the interaction with light, cholesteric polymer scaffolds (templates) filled with azobenzene-containing LC polymer have

been developed. The possibility to use them as a media for holographic recording of diffraction gratings has been demonstrated. Besides the transmission gratings we have managed to create reflection gratings with the opposite handedness in respect to the natural helical architecture, which enables two-color wavelength-selective mirrors.

In **Figure 1** the fabrication procedure of the composite films is schematically depicted (details are in the Experimental Section). The first step consists in the preparation of photopolymerizable cholesteric layer with planar orientation (helix axis z is perpendicular to the film plane) composed of a mixture of mesogenic mono- and diacrylates, low-molar-mass LCs, a chiral dopant, and a photoinitiator (**Figure 2**). Photopolymerization and the removal of all low-molar-mass components result in a porous cholesteric polymer network or "sponge-like" photonic scaffold/container. Such continual porous polymer structure can be filled with either low-molar-mass or polymeric compounds. The cholesteric scaffold was filled with the azobenzene-containing LC side-chain copolymer PAAzo (Figure 2). The resulted composite films were used for holographic recording of diffraction gratings. The polymer PAAzo has been established as a material allowing high photoinducible birefringence (or dichroism)[45,46] and was used as an active optical media for lasing.[33,47]

As shown in Figure 1, the illumination of the composite film with linearly polarized light leads only to a uniaxial orientation
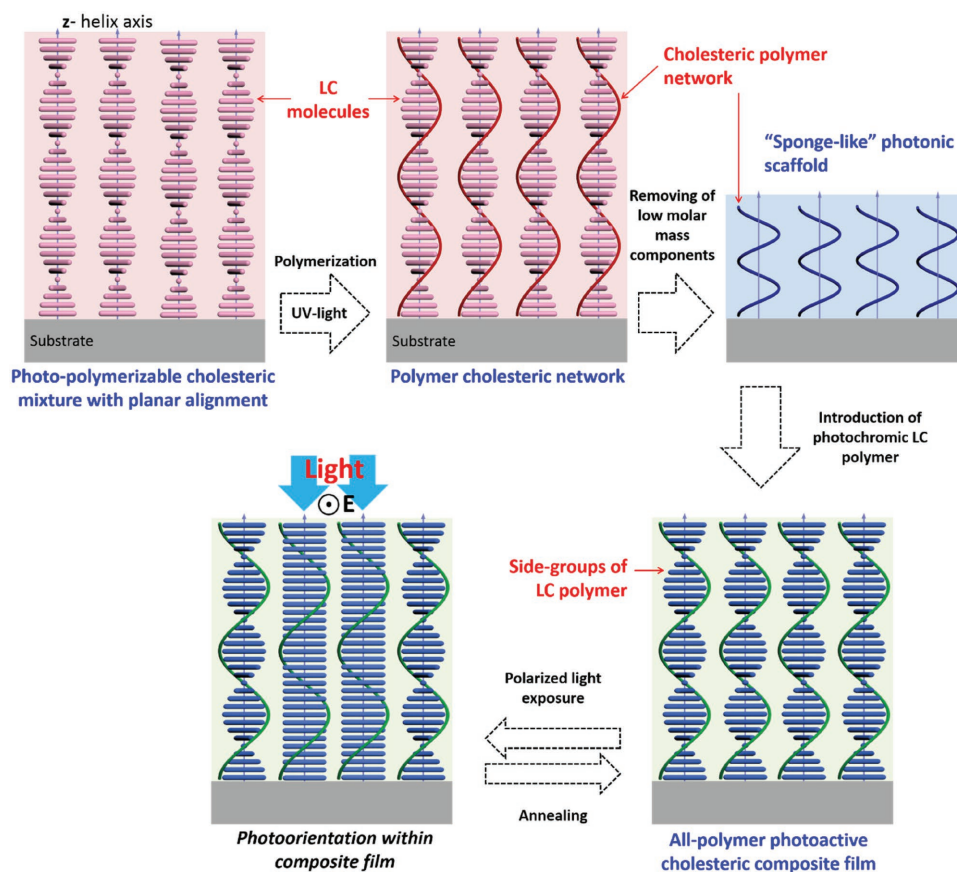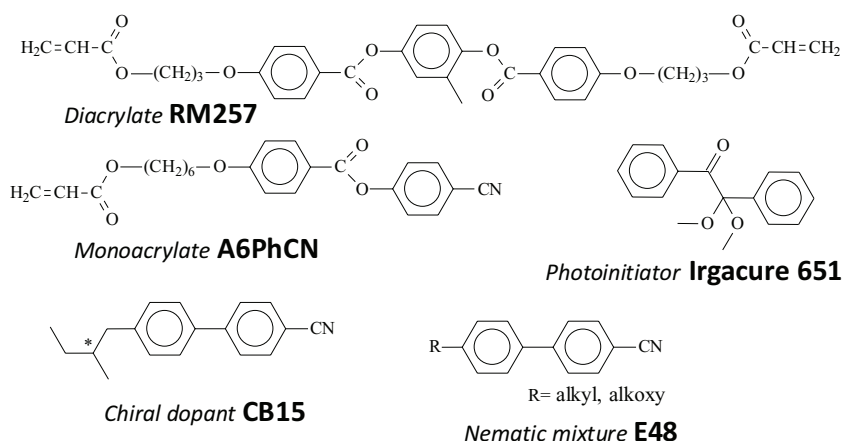

Figure 1. Schematic representation of the preparation procedure of cholesteric composite films. All low-molar-mass components of photopolymerizable mixture are presented in one color (red) as well as all the side groups of LC polymer (blue); polymer backbone and spacers are omitted.

1700314 (2 of 10)

**ADVANCED
SCIENCE NEWS**

www.advancedsciencenews.com

**ADVANCED
OPTICAL
MATERIALS**

www.advopticalmat.de

Components of photopolymerizable cholesteric mixtures

Diacrylate **RM257**

Monoacrylate **A6PhCN**

Photoinitiator **Irgacure 651**

Chiral dopant **CB15**

R= alkyl, alkoxy

Nematic mixture **E48**

Photosensitive nematic copolymer

PAAzo

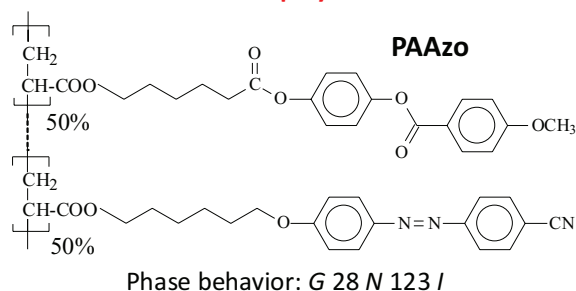Phase behavior: *G* 28 *N* 123 *I*

Figure 2. Chemical structures of low-molar-mass substances and azobenzene-containing copolymer PAAzo used for the composite films preparation.

of the side-chain fragments of the embedded LC polymer while the cholesteric helical structure remains unchanged since it is imprinted in the covalently crosslinked polymer network. Thus, the proposed approach allows independent use of both: (i) the advantages of azobenzene-containing LC polymer and (ii) unique optical properties of cholesteric structure preserved in polymer scaffold in order to create "smart" materials for optics.

2. Results and Discussions

2.1. Optical Properties of the LC Composite Films

Two different photopolymerizable monomer mixtures whose compositions are shown in **Table 1** were used to create the cholesteric photonic scaffolds. The mixtures were made by mixing together a nematic liquid crystal E48, a chiral dopant CB15 inducing right-handed helix, nematic mono- and diacrylates and

a small amount of the UV photoinitiator Irgacure 651. The photopolymerized Sample 1 possesses low crosslinking density (8%) and contains the nematic monoacrylate A6PhCN, whereas Sample 2 is highly crosslinked (49%) and does not contain a monoacrylate. The planar oriented layers of the prepared polymerized cholesteric mixtures exhibit selective light reflection band at 600 and 850 nm, respectively. A reasonable shrinkage of the cholesteric networks accompanied by a quite strong shift of the reflection band toward the UV region (Figure S2, Supporting Information) is observed after removing of all low-molar-mass components by washing with ethanol. The shrinkage of cholesteric network is schematically depicted in the Figure 1. The scanning electron microscopy (SEM) and atomic force microscopy (AFM) studying of the "empty" scaffolds revealed porous "sponge-like" structure with the pores size less than 100 nm as illustrated in Figure S4 (Supporting Information). The resulted sponge-like scaffold or container was swollen in the isotropic melt of the LC copolymer PAAzo at 130 °C (see Figure 2) in order to reduce the viscosity of polymer melt and consequently to speed up this processing step. The wavelength of the reflection peak of the films after the PAAzo introduction increases up to 510 and 690 nm for Samples 1 and 2, respectively. The observed equilibrium values of helix pitches are smaller than these values immediately after photopolymerization of cholesteric scaffolds. The difference can be associated with the incomplete filling of the cholesteric network due to the fact that isotropic melt of PAAzo is a worse solvent for the anisotropic network in comparison to E48.[48]

The thermo-optical measurements of the composite films have revealed the gradual red shift of the reflection peak and the threshold-like decrease in the bandwidth (Figure S3, Supporting Information) attributed to the isotropization of the introduced LC polymer PAAzo resulting in the reduction of birefringence and, consequently, in the narrowing of the reflection band (Equation (2)). The increase of temperature above 150 °C causes the sweating of PAAzo onto the film surface with a corresponding blue shift of the reflection maximum and decreases its bandwidth (Figure S3).

Thus, photopolymerization of the cholesteric mixtures followed by removal of low-molar-mass components and refilling

Table 1. The compositions of photopolymerizable mixtures for the preparation of cholesteric scaffolds.

	Composition of photopolymerizable cholesteric mixture[a] [wt%]				λ^1_{max}[b] [nm]	λ^2_{max}[c] [nm]
	E48	CB15	A6PhCN	RM257		
Sample 1	52	25	14	8	600	510
Sample 2	30	20	–	49	850	690

[a]All mixtures contain 1 wt% of photoinitiator Irgacure 651; [b]λ^1_{max} is selective light reflection maximum after photopolymerization of cholesteric mixture; [c]λ^2_{max} is selective light reflection maximum after filling with LC polymer PAAzo.

**ADVANCED
SCIENCE NEWS**

www.advancedsciencenews.com

**ADVANCED
OPTICAL
MATERIALS**

www.advopticalmat.de

with azobenzene-containing copolymer makes it possible to obtain new type of photochromic polymer–polymer composites having helical supramolecular structure and selective light reflection in the visible spectral range.

2.2. Photo-Orientation in the LC Composite Films under Polarized Light Action

It is well known that under the action of linearly polarized light a cyclic reversible E–Z–E isomerization of azobenzene fragments takes place. Due to the angular-selective character of light absorption, following numerous repetitive isomerization cycles the azobenzene groups become uniaxially oriented in a plane perpendicular to the electric field vector of the incident light. As shown previously, the nonphotochromic mesogenic groups included in the azo-containing copolymers also become oriented along with the azobenzene moieties.[45] Thus, by virtue of the cooperative character of the orientation process very strong photoinduced optical anisotropy can be reached. This phenomenon underlies the use of this kind of polymers for optical recording and can result in their bulk (molecular) alignment.

To study the photoorientation processes, a linearly polarized laser beam of 532 nm and intensity of ≈9.8 mW cm^{-2} was used. Here we present the results of the study of Sample 2, as there is no overlap of the absorption band of azopolymer and selective reflection of the cholesteric network, which will clearly show the changes in optical properties. It is worth mentioning that the selected laser wavelength plays a dual role, on one hand, it effectively induces the photo-orientation process providing

preferential formation of the E-form of azobenzene fragments, and on the other hand, it is relatively weakly absorbed promoting uniform distribution of light intensity across the film thickness.

Figure 3a,b shows the polarized transmittance spectra for the parallel and the perpendicular light components with respect to the direction of the molecular orientation. The spectra show a growth of the left peak shoulder of the parallel component, whereas the opposite behavior is observed for the perpendicular one. The spectral changes in the range of the photonic band gap structure are associated with uniaxial alignment of the mesogenic groups under polarized light action.

Despite on high absorption of the sample we were able to estimate the value of the linear dichroism (D) at 460 nm which corresponds to the n–π* transition of the azobenzene groups. The dichroism values were calculated from the spectra using Equation (3)

$$D = (A_\parallel - A_\perp)/(A_\parallel + A_\perp) \tag{3}$$

where $A_\parallel$ and $A_\perp$ is polarized absorbance along and perpendicular to the preferred chromophores orientation, respectively. Figure 3c shows the kinetic curve of the dichroism growth, i.e., the orientation of azobenzene side fragments of LC copolymer. The inserted polar diagram also clearly demonstrates that the molecular orientation takes place in the direction perpendicular to the polarization plane of laser light.

In addition we have demonstrated the possibility of using polarized light for photopatterning. Figure 3d shows the optical pattern recorded on Sample 2 by irradiation with linearly polarized light through a mask (cupper grid for electron microscopy,
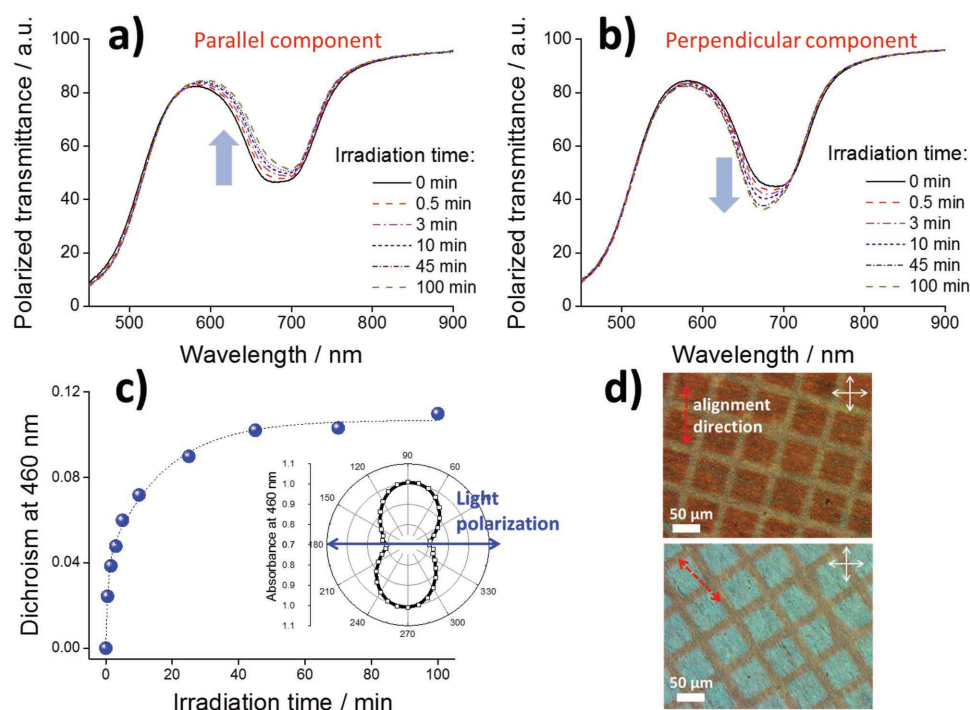

Figure 3. Evolution of polarized transmittance spectra of Sample 2 under the action of linearly polarized laser light with the wavelength of 532 nm a,b) and a corresponding linear dichroism growth c); polarized optical image of the film irradiated through the metal grid d). Polarizer and analyzer are indicated by the crossed white arrows. The parallel and perpendicular components of the polarized light absorbance are provided in respect to the molecular alignment direction.

ADVANCED
SCIENCE NEWS
www.advancedsciencenews.com

ADVANCED
OPTICAL
MATERIALS
www.advopticalmat.de

Table 2. Schematic representation of spatial polarizations distributions across the grating vector. RCP is right-circularly polarized light; LCP is left-circularly polarized light. Intensity of light is indicated by the length of the arrow.

	Polarization sates of the interfering beams	Spatial distribution of polarization across the grating vector				
		0	Λ/4	Λ/2	3Λ/4	Λ
Intensity interference pattern (IIP)	p- p-	↔	↔	◇	↔	↔
Polarization interference pattern (PIP)	RCP LCP	↔	↗	↕	↘	↔

mesh 400). By rotating the exposed sample between crossed polarizers it is seen that the irradiated areas become dark or bright depending on the angle between the analyzer and the direction of molecular alignment which underlines the effectiveness of orientational photopatterning.

Thus, in the composites under study it is possible to create additional optical anisotropy by polarized light exposure while the cholesteric helical structure does not collapse and preserves its properties even after a long-time light exposure. This fact is crucial for recording of polarization (orientation) gratings in the cholesteric composite films.

2.3. Transmission Holographic Gratings Recording in the LC Composite Films

To record the transmission diffraction gratings, the interference pattern of two coherent laser beams (532 nm) of equal intensity with parallel polarizations (*p-p*) as well as two beams with right- and left-circular polarizations (RCP and LCP) have been used. As shown in **Table 2** (see the Experimental Section), the interference of two beams with parallel *p* polarization leads to the intensity interference pattern (IIP) that is spatial distribution of the light intensity, the polarization remains constant. On the other hand, the interference of two opposite circularly polarized beams provides the polarization interference pattern (PIP) i.e. a spatial modulation of the polarization state maintaining a constant intensity.

In the first set of experiments Sample 1 was exposed to IIP and PIP. **Figure 4**a shows the growth of the diffraction efficiency of the first diffraction order. As clearly seen, the grating recorded by PIP is about twice as effective as IIP. The optical micrograph of the polarization grating recorded by PIP exposure is depicted in **Figure 5**a,b. The regions of the sample with and without the grating are clearly visible in Figure 5a. Figure 5b shows a magnified fragment of the recorded gratings
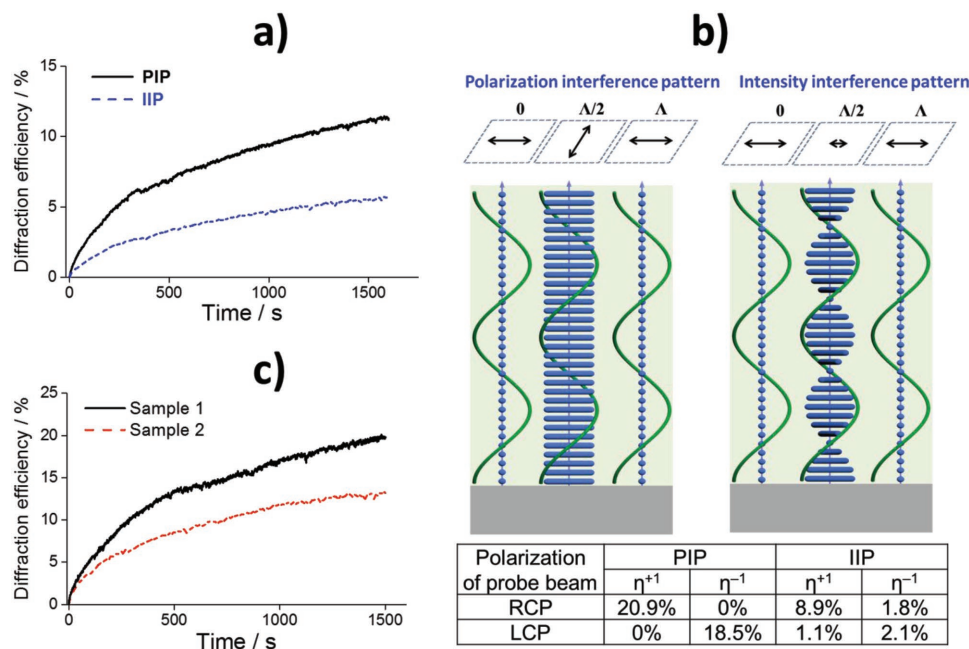

Polarization	PIP		IIP	
of probe beam	η^{+1}	η^{-1}	η^{+1}	η^{-1}
RCP	20.9%	0%	8.9%	1.8%
LCP	0%	18.5%	1.1%	2.1%

Figure 4. The growth of the diffraction efficiency under exposure of Sample 1 to the polarized interference pattern (PIP) and to the intensity interference pattern (IIP) a); schematic representation of both gratings recorded in Sample 1 and corresponding diffraction efficiencies of +1st (η^{+1}) and −1st (η^{-1}) diffraction orders b). Diffraction efficiency growth of Samples 1 and 2 under exposure to PIP c).

ADVANCED
SCIENCE NEWS
www.advancedsciencenews.com

ADVANCED
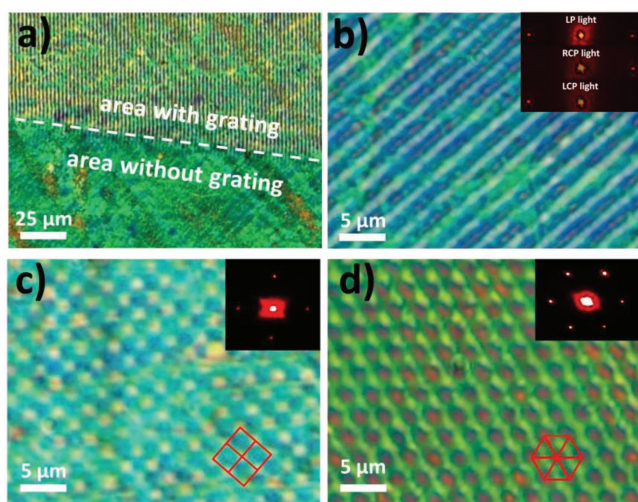OPTICAL
MATERIALS
www.advopticalmat.de

Figure 5. Polarized optical images of 1D sinusoidal a,b), 2D square c), and hexagonal d) gratings inscribed in Sample 1 by exposure to the polarized interference pattern (PIP). Insets in (b) show the diffraction light patterns of the probe laser beam of linear (LP) and right- and left-circular (RCP and LCP) polarization. Insets in (c) and (d) display the diffraction patterns of a linearly polarized probe beam.

with alternating parallel lines, which correspond to the areas of different molecular orientation. The grating period matches the geometry of the holographic experiment (the angle between the interfering laser beams was 14.5°) and equals about 2.1 µm.

It should be noted that the specific features of the diffraction of the probe beam depend on its polarization state. If the input light is linearly polarized, two diffraction orders are observed (+1st and −1st), whereas for the circularly polarized light diffraction occurs only in the one order (+1st or −1st) as shown in the insets in Figure 5b. The reasons for such discrepancy are described in detail in.[49–51] The results demonstrate that the fabricated grating is a pure polarization grating (or in other words the orientation grating)[49,50] i.e., orientation of the side fragments of PAAzo follows the polarization distribution of the interference pattern. This case is displayed schematically in Figure 4b. Here we also note that the cholesteric helical structure of the scaffold is maintained constant. The values of the diffraction efficiencies for RCP and LCP light are gathered in the table in Figure 4b. The photoinduced birefringence (Δn) of the PIP grating for circular polarized probe beam was estimated using diffraction efficiency values (η) according to Equation (4)[51]

$$\eta = \sin^2\left[\frac{\pi \Delta n d}{\lambda}\right] \tag{4}$$

where d is film thickness and λ is a probe beam wavelength. The values of Δn were estimated as 0.011 and 0.010 for RCP and LCP probe beams, correspondingly, which is in accordance with Δn values for pure copolymer PAAzo reported previously.[47]

The exposure of Sample 1 to IIP results in the orientation of the side fragments of LC copolymer taking place mainly in the areas of constructive interference (i.e., in the areas of a maximum intensity), while in the regions of destructive interference (the areas of a minimal light intensity) the orientation processes are suppressed as it is schematically shown in Figure 4b. This fact is supported by the diffraction efficiency dependence on the polarization state of the probe beam (see Table in Figure 4b). It can be seen that regardless of the polarization of the probe beam, diffraction occurs in two orders, and only one of them is more effective than the other. The maximal diffraction efficiency is achieved with RCP light, which is in accordance with the handedness of cholesteric helical structure of polymer scaffold which is also right-handed.

In addition to the 1D transmission gratings the 2D gratings have been also successfully recorded. 2D square and hexagonal gratings have been fabricated by a two-step (after each exposure step the sample was rotated by 90°) or a three-step (rotated by 60°) illumination of the sample with PIP. The two-step exposure for 25 and 1 min yielded square grating as it was confirmed by the polarized optical microscopy and by diffraction pattern (Figure 5c). The three-step exposure for 25, 4.5, and 0.7 min resulted in a hexagonal grating as shown in Figure 5d. The efficiency of the 2D gratings can be varied by purposeful dividing the dynamic range of the material, i.e., by varying the illumination dose at each exposure step.

It is important to emphasize that the AFM study of the surfaces of the samples after a long-time gratings recording has revealed no surface relief formation (Figure S5, Supporting Information) as it would be expected for nonconfined azobenzene-based polymer films. This fact shows that the polymer network of cholesteric scaffold prevents photoinduced mass-flow (or mass-transfer) of azobenzene polymer embedded in it, and once again confirms the formation of orientation gratings.

Let us briefly compare the behavior of Sample 1 and Sample 2 during holographic gratings recording. For this purpose two samples were exposed to PIP, while monitoring the probe beam had a right circular polarization. Figure 4c shows the recording curves for the first diffraction order which is the only order of diffraction for given polarization state of the probe beam. It was revealed that Sample 1 has higher diffraction efficiency than Sample 2. This may be due to lower crosslinking density of cholesteric scaffold of Sample 1 and higher content of photochromic copolymer PAAzo (see Table 1).

Another very important feature of all gratings described above is that they can be easily erased by an annealing above the glass transition temperature of the LC polymer embedded in the cholesteric scaffold. Typical curves of the reduction of diffraction signal during annealing at 50 °C are presented in Figure S6 (Supporting Information). The cholesteric network plays a key role in this process, since at elevated temperatures it acts as a template with memory effect and causes the adjustment/alignment of the LC fragments of PAAzo in a helical structure thereby completely destroying the photoinduced order.

Thus, proposed materials allows creating 1D and 2D transmission diffraction gratings associated only by modulation of refractive index, herewith maintaining selective light reflection from a cholesteric superstructure. The composites are suitable for multiple recording/erasure cycles which are highly required for practical applications.
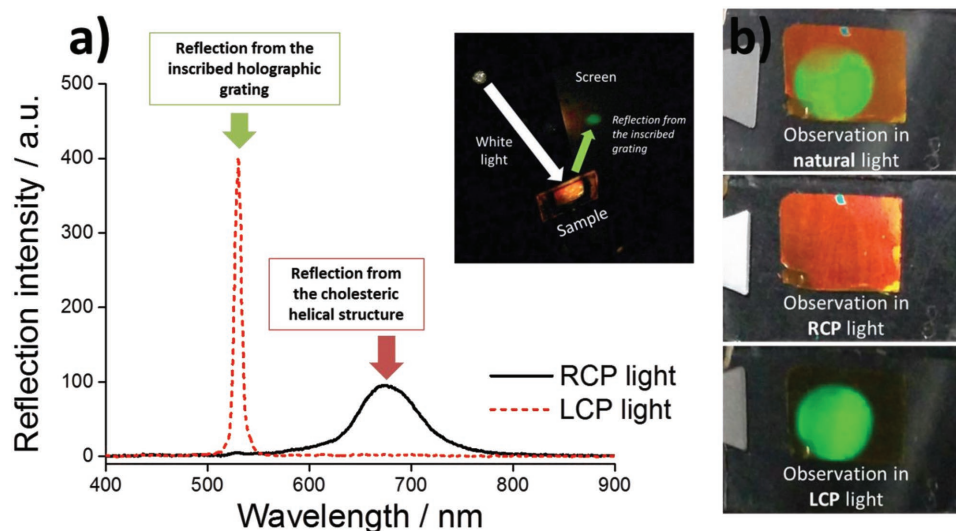
**ADVANCED
SCIENCE NEWS**
www.advancedsciencenews.com

**ADVANCED
OPTICAL
MATERIALS**
www.advopticalmat.de

Figure 6. Right- and left-circular polarized reflection spectra of Sample 2 with the reflection grating inscribed by IIP exposure of two LCP laser beams a). Inset shows a white light selective reflection. Images of Sample 2 were obtained in natural, RCP and LCP light b).

2.4. Recording of Holographic Reflection Gratings in LC Composite Films

There is a very limited number of works devoted to the reflection gratings in azobenzene based polymer systems. In 2001 Eichler et al. demonstrated the ability to record reflection gratings in thick (≈50 µm) azopolymer layers using holographic exposure.[52] A year later, Nikolova et al. holographically inscribed polarization reflection gratings in the azobenzene-doped gelatin films but stability and efficiency of the gratings were poor.[53] It is noteworthy that the reflection gratings in cholesterics present a special interest because they combine on the one hand cholesteric structure possessing intrinsic selective light reflection with definite circular polarization of wavelength of the reflected light and on the other hand holographic reflection gratings with fine tunable optical parameters. In the current work we have realized the reflection gratings holographically recorded in cholesteric polymer systems containing azobenzene side groups.

The feature of the reflection gratings recording is that two laser beams propagate in opposite directions and overlap in the sample resulting in an interference pattern where the grating vector is perpendicular to the sample plane in contrast to the transmission gratings where grating vector lays in the sample plane. It is also known that the exposure of azobenzene LC systems to circular-polarized light leads to a circular optical anisotropy (Δn_{cir}, circular photoinduced birefringence) by analogy with the optical anisotropy arising due to the linearly polarized light illumination.[54–56] Hence, we decided to exploit the interference of two laser beams with the same circular polarization, either right- or left-handed. This results in a spatial modulation of light intensity across the film thickness at constant polarization state (by analogy with IIP exposure in Table 2). The main goal of this experiment was to create an artificial photonic structure or a selective mirror similar to the natural cholesteric helical structure.

To clearly separate the reflection of a cholesteric superstructure (which occurs perpendicularly to the film plane) and that

of a holographically fabricated grating, the exposure configuration in which one beam directed to the normal of the sample surface and the opposite directed beam slanted to the sample by an angle of 20° to the normal was used.

The exposure of Sample 2 to LCP laser beams for 10 min results in a reflection grating with the efficiency of about 10% at the wavelength of 532 nm. As shown in **Figure 6**a the formed grating is selective to LCP light, which matches to the polarization state of the recording beams while the helical structure of the polymer scaffold selectively reflects RCP light. The reflection peak corresponds to the used laser wavelength and is equal to 532 nm. The geometry of holographic experiment allows spatially separating the reflection of the inscribed grating and that of the natural cholesteric structure (see inset in Figure 6a). It is noteworthy that the width of reflection peak of the recorded grating is of about 9 nm which is one order of magnitude lower than that for the cholesteric reflection peak (≈80 nm). It means that such gratings could be potentially used as notch-filters. The optical feature of the grating is clearly seen from the images presented in Figure 6b. By observation of the grating with natural (nonpolarized) light one can see two colors simultaneously, green and red, belonging to the recorded grating and to that of the cholesteric basic structure, respectively. If white light is right-circularly polarized, only the reflection color from the cholesteric scaffold is visible. On the contrary, in LCP light the green reflection of the recorded grating can be detected only.

An exposure to two RCP beams provides reflection grating selective to RCP light. These results as well as the data concerning the reflection grating in Sample 1 are presented in Supporting Information (Figure S7). The recorded reflection gratings are stable in time and can be erased by annealing. The diffraction efficiency of the gratings is usually in the range 3%–11% (for appropriate circular polarized light) and strongly depends on the quality of the used film. As for the transmission gratings the fabrication of the reflection ones does not change the surface topology of the film at all (Figure S5b, Supporting Information). It is worth to note that the reflection gratings are

**ADVANCED
SCIENCE NEWS**
www.advancedsciencenews.com

**ADVANCED
OPTICAL
MATERIALS**
www.advopticalmat.de

characterized by much higher spatial frequency/resolution (in our case ≈166 nm, taking into account average refractive index of about 1.6) than related transmission-type gratings (submicrometer resolution).

Thus, the selective reflection gratings mimicking natural optical properties of cholesteric supramolecular structure were successfully fabricated. The simultaneous existence of cholesteric structure and all-optically formed artificial photonic structure was demonstrated. It is important to mention, that the cholesteric scaffold properties can be purposefully programmed at early stages of production process e.g., by adjustment of cholesteric monomer mixture or by the photopolymerization conditions. On the other hand, the properties of reflection gratings can also be tuned by the geometry of holographic recording as well as by the polarization states of the recording laser beams. These facts make the proposed materials a versatile tool for various photonic and optical applications.

2.5. Formation of Multicolored Images in LC Composite Films

The proposed versatile approach and the related materials could likely be used not only for diffractive optics and optical data storage but could also be a candidate for the optical security devices and anticounterfeiting tags of high protection level.[57,58] Recently, the potential of cholesteric materials in spherical confinement as security devices with physical unclonable functions has been demonstrated.[59] In the current chapter we will show our preliminary results and will give an outlook on this topic.

A photopolymerizable mixture similar to that of Sample 2 but with higher concentration of the chiral dopant (≈30 wt%) was prepared. The planar oriented layer of this mixture has been irradiated with UV light in two steps: firstly, through the mask (a positive mask with the Fraunhofer Institute abbreviation, Fh-IAP) for 2 min and then homogeneously without a mask for 15 min. This approach was previously used and allows obtaining an optical pattern exhibiting various colors (due to various helical pitches) due to low-molar-mass component migration and variation of the crosslinking density of cholesteric polymer network.[60,61] In our case, the areas corresponding to the letters have a lower degree of crosslinking and, consequently, a reflection at shorter wavelengths. After photopolymerization and removal of low-molar-mass components, the cholesteric container was filled with polymer PAAzo (the images of the sample after each production step are provided in Figure S8a, Supporting Information). Higher amount of polymer penetrates in the regions of a low crosslinking density compared to highly crosslinked areas; thereby, the pattern containing high concentration of PAAzo appears in the film that is clearly demonstrated in Figure S8b.

After that the reflective grating selective to LCP light was recorded by exposure to two LCP laser beams for 10 min. **Figure 7** (at the left) shows the image of the resulting sample observed with RCP light. A two-color picture corresponds to the selective light reflection from cholesteric helical structure with a patterned helix pitch. If the observation is carried out with LCP light the image formed by a cholesteric preprogrammed scaffold is invisible, whereas the holographically recorded reflection grating becomes visible (Figure 7, at the right). Since the areas
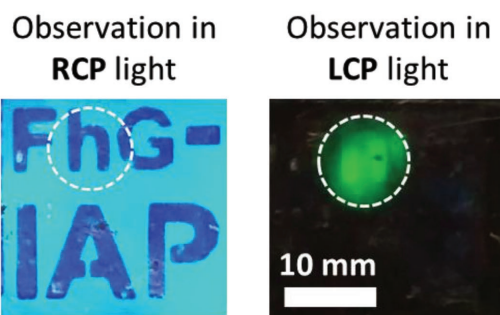

Figure 7. Images of the demonstration sample made in right- and left-circular polarized (RCP and LCP) light. A dashed round area corresponds to the region of a holographically recorded reflection grating.

of "the letters" are rich with azobenzene-containing LC polymer the efficiency of the reflection grating in these areas is higher as evidenced by brighter green color.

In general, it is possible to create multicolored images by purposeful manipulation of the helix pitch of the cholesteric polymer scaffolds. The reflection color of the grating can also be tuned by varying the angle between the recording beams and/or by using other recording wavelengths. Moreover, the reflection gratings can be easily patterned using the photomasks. All these ways of tuning/adjustment of the proposed materials allow considering them as perspective "smart" materials for optical recording and security purposes.

3. Conclusion

Novel LC polymer composites based on cholesteric polymer scaffolds filled with an azobenzene-containing LC polymer were elaborated. Polarized light exposure brings unidirectional molecular alignment of LC polymer side-groups without any distortion of the helical supramolecular structure of the cholesteric scaffold which enables to keep unique optical properties of a cholesteric mesophase like selective light reflection and to manipulate independently the orientation of the LC polymer. These materials were successfully utilized for optical recording of 1D and 2D transmission diffraction gratings by holographic exposure to polarization or intensity interference patterns. The gratings obtained can be classified as polarization diffraction gratings. The gratings are rewritable, they can be thermally erased and another structure can be inscribed again. Furthermore, holographic fabrication of reflection gratings in cholesteric material was demonstrated for the first time. The reflection gratings possess higher spatial resolution (≈166 nm) compared to the transmission one, and they are strongly selective to circularly polarized light which is predetermined by the polarization states of the recording laser beams. Possible application of new composite materials for optical security features using holographic patterning of the reflection gratings having polarization selectivity opposite to the cholesteric structure is proposed. The presented class of "dual" optical materials is effective and versatile and can be easily applied to a broad variety of polymeric materials (amorphous or liquid crystalline) with specific properties. The rich toolbox for the adjustment and material preprograming combined high performance

**ADVANCED
SCIENCE NEWS**
www.advancedsciencenews.com

**ADVANCED
OPTICAL
MATERIALS**
www.advopticalmat.de

optical properties allows considering them as candidate for modern optics.

4. Experimental Section

Materials: Acrylic LC monomer A6PhCN were obtained as previously described in ref. [62]. Nematic diacrylate RM257, chiral dopant CB15, and nematic mixture E48 were purchased from "Merck." Radical UV photoinitiator Irqacure651 was purchased from "Ciba." The copolymer PAAzo with a molar ratio of mesogenic and azobenzene side groups of 1:1 was synthesized by free radical polymerization of appropriate monomers which have been obtained according to procedures described in ref. [45]. The reaction was carried out in anhydrous benzene in a sealed tube under argon atmosphere with the initiator AIBN (2 wt%) for 100 h at 70 °C. The polymerization was carried out to high conversions. The copolymer was purified by repeated extraction with hot methanol and dried in vacuum at 50 °C. M_w of PAAzo was about 8.6 kDa ($M_w/M_n \approx 1.6$) which was determined by GPC using a "Knauer" chromatograph (UV detector, column type "LC-100" with a sorbent 1000 Å; solvent THF, 1 mL min^{-1}; 25 °C; polystyrene standard). Phase transition temperatures were detected by polarized optical microscopy ("POLAM-R-112") equipped with a heating stage ("Mettler FP-86"), as well as differential scanning calorimetry ("Mettler TA-4000," heating rate 10 K min^{-1}).

The cholesteric photopolymerizable mixtures of different compositions were prepared by dissolving appropriate amounts of the components (Table 1) in chloroform. Then the solvent was slowly evaporated and the residue was dried in vacuum at 50 °C for several hours.

Sample Preparation: Glass sandwich-like cells with the thickness of 10 µm were used for cholesteric polymer films preparation. In order to improve adhesion of polymer network one of the glass substrates was preliminary functionalized by 3-(trimethoxysilyl)propyl methacrylate,[14] whereas another was treated with triethoxy(octyl)silane to decrease adhesion to the glass.[27] The fresh-prepared cholesteric monomer mixtures have been introduced into the cells at room temperature. The mixtures were planarly aligned by shear forces followed by photopolymerization using UV lamp (the spectral range is 345–355 nm, exposure time is 10 min., intensity is 12 mW cm^{-2}). After polymerization and removal of one glass plate (the hydrophobically functionalized one) the cholesteric polymer film was thoroughly washed in ethanol in order to get rid of all low-molar-mass components and then dried at room temperature for several hours.

During the final stage the photochromic nematic copolymer PAAzo was introduced into the cholesteric polymer network at 130 °C (in isotropic state) by capillary forces. The excess of the polymer melt was gently removed from the surface with nonwoven tissue. Then the sample was slowly cooled down to the room temperature. The resulted thickness of Sample 1 and 2 was 8.95 and 8.07 µm, respectively.

Optical Structuring: Holographic exposure technique was applied for the fabrication of transmission and reflection diffraction gratings. The transmission gratings were recorded by means of a symmetric exposure of the intensity interference pattern (IIP) of two mutually coherent *p*-polarized beams of equal intensities or to the polarization interference pattern (PIP) formed by RCP and LCP beams (Table 2). Quarter-waveplates were used for obtaining circular polarization of the light. Recording intensity was about 100 mW cm^{-2}. The scheme of a holographic setup is provided in Figure S1a (Supporting Information). A DPSS laser (Elforlight) operating at a wavelength of 532 nm was used as a coherent light source. The grating period, Λ, was dictated by the angle between the interfering beams and has been set to 2.1 µm. A nonactinic probe beam from an He–Ne laser at $\lambda_t = 632.8$ nm with an output power of 15 mW (Thorlabs) was used for a real-time monitoring of the transmission grating formation. Polarization of an He–Ne probe laser beam in all cases was parallel to the gratings fringes, unless otherwise mentioned. The transmission gratings fabricated in the current work

operate in Raman–Nath regime ("thin" diffraction gratings) which is characterized by the presence of multiple diffracted orders. The diffraction efficiency (η) of the transmission gratings was determined for the first order as a ratio between of intensity of the diffracted beam and intensity of the input beam.

The reflection gratings were inscribed using the exposure configuration shown in Figure S1b (Supporting Information). In this case the recording beams were directed from the opposite sites on the sample. One beam was directed to a normal of a sample surface and the second, opposite beam was slanted to the sample by the angle of 20° to a normal. The samples were exposed with the interference pattern of two laser beams with right- or left circular polarization. Such configuration provides spatial modulation of intensity of RCP or LCP light, respectively (analogues to IIP in Table 2).

Measurements: The absorption spectra were measured using a spectrometer TIDAS (J&M). For the polarized light absorbance measurements spectrometer was equipped with a polarizer (Glan-Taylor prism) or with the stack of a polarizer and an achromatic $\lambda/4$-waveplate. The optical axis of waveplate was rotated by +45°/−45° with respect to the axis of the polarizer in order to produce left/right circularly polarized light, respectively. The intensity of the laser light was measured by a power meter PM-100D (Thorlabs). The polarized optical microscopic investigations were performed using a microscope AxioPlan2 (Carl Zeiss). Film thickness was measured by profilometer Dektak 150 (Veeco). The surface relief topography of the films was studied by atomic force microscopy SPM Smena (NT-MDT) performed in the tapping mode. The SEM measurements were carried out with microscope Neon 40 (Carl Zeiss). Samples were imaged with the following parameters: electron beam energy, 3.00 kV; aperture size, 30 µm; signal, SE2.

Supporting Information

Supporting Information is available from the Wiley Online Library or from the author.

Conflict of Interest

The authors declare no conflict of interest.

[1] G. Chilaya, *Cholesteric Liquid Crystals: Properties And Applications*, Lambert Academic Publishing, Saarbrücken, Germany, **2013**.

**ADVANCED
SCIENCE NEWS**

www.advancedsciencenews.com

**ADVANCED
OPTICAL
MATERIALS**

www.advopticalmat.de

[2] H. K. Bisoyi, Q. Li, *Chem. Rev.* **2016**, *116*, 15089.

[3] K. M. Lee, V. P. Tondiglia, T. J. White, *Soft Matter* **2016**, *12*, 1256.

[4] H. Khandelwal, M. G. Debije, T. J. White, A. P. Schenning, *J. Mater. Chem. A.* **2016**, *4*, 6064.

[5] M. Mitov, N. Dessaud, *Nat. Mater.* **2006**, *5*, 361.

[6] N. Katsonis, E. Lacaze, A. Ferrarini, *J. Mater. Chem.* **2012**, *22*, 7088.

[7] Y. Li, C. Xue, M. Wang, A. Urbas, Q. Li, *Angew. Chem., Int. Ed.* **2013**, *52*, 13703.

[8] H. K. Bisoyi, Q. Li, *Angew. Chem., Int. Ed.* **2016**, *55*, 2994.

[9] S. Iamsaard, S. J. Aßhoff, B. Matt, T. Kudernac, J. J. Cornelissen, S. P. Fletcher, N. Katsonis, *Nat. Chem.* **2014**, *6*, 229.

[10] *Cross-Linked Liquid Crystalline Systems* (Eds: D. Broer, G. Crawford, S. Zumer), CRC Press, Boca Raton, FL, USA, **2011**.

[11] *Liquid Crystalline Polymers* (Eds: V. Thakur, M. Kessler), Springer, Cham, Switzerland, **2016**.

[12] J. E. Stumpel, D. J. Broer, A. P. Schenning, *Chem. Commun.* **2014**, *50*, 15839.

[13] D. Liu, D. J. Broer, *Langmuir* **2014**, *30*, 13499.

[14] J. E. Stumpel, E. R. Gil, A. B. Spoelstra, C. W. Bastiaansen, D. J. Broer, A. P. Schenning, *Adv. Funct. Mater.* **2015**, *25*, 3314.

[15] J. E. Stumpel, C. Wouters, N. Herzer, J. Ziegler, D. J. Broer, C. W. Bastiaansen, A. P. Schenning, *Adv. Opt. Mater.* **2014**, *2*, 459.

[16] A. Bobrovsky, P. Samokhvalov, V. Shibaev, *Adv. Optical Mater.* **2014**, *2*, 1167.

[17] D. Liu, D. J. Broer, *Angew. Chem., Int. Ed.* **2014**, *53*, 4542.

[18] D. Y. Kim, C. Nah, S. W. Kang, S. H. Lee, K. M. Lee, T. J. White, K. U. Jeong, *ACS Nano* **2016**, *10*, 9570.

[19] C. D. Hasson, F. J. Davis, G. R. Mitchell, *Chem. Commun.* **1998**, *22*, 2515.

[20] M. K. Khan, A. Bsoul, K. Walus, W. Y. Hamad, M. J. MacLachlan, *Angew. Chem.* **2015**, *127*, 4378.

[21] M. E. McConney, V. P. Tondiglia, J. M. Hurtubise, T. J. White, T. J. Bunning, *Chem. Commun.* **2011**, *47*, 505.

[22] V. M. Zamarion, M. K. Khan, M. Schlesinger, A. Bsoul, K. Walus, W. Y. Hamad, M. J. MacLachlan, *Chem. Commun.* **2016**, *52*, 7810.

[23] S. M. Wood, J. A. J. Fells, S. J. Elston, S. M. Morris, *Macromolecules* **2016**, *49*, 8643.

[24] N. Herzer, H. Guneysu, D. J. Davies, D. Yildirim, A. R. Vaccaro, D. J. Broer, C. W. M. Bastiaansen, A. P. Schenning, *J. Am. Chem. Soc.* **2012**, *134*, 7608.

[25] D. J. Mulder, A. P. Schenning, C. W. M. Bastiaansen, *J. Mater. Chem. C* **2014**, *2*, 6695.

[26] M. Moirangthem, R. Arts, M. Merkx, A. P. Schenning, *Adv. Funct. Mater.* **2016**, *26*, 1154.

[27] A. Ryabchun, I. Raguzin, J. Stumpe, V. Shibaev, A. Bobrovsky, *ACS Appl. Mater. Interfaces* **2016**, *8*, 27227.

[28] A. Bobrovsky, V. Shibaev, J. Wendorff, *Liq. Cryst.* **2007**, *34*, 1.

[29] A. Ryabchun, A. Bobrovsky, Y. Gritsai, O. Sakhno, V. Shibaev, J. Stumpe, *ACS Appl. Mater. Interfaces* **2015**, *7*, 2554.

[30] A. Ryabchun, A. Bobrovsky, A. Sobolewska, V. Shibaev, J. Stumpe, *J. Mater. Chem.* **2012**, *22*, 6245.

[31] A. Ryabchun, A. Bobrovsky, J. Stumpe, V. Shibaev, *Adv. Opt. Mater.* **2015**, *3*, 1462.

[32] A. Ryabchun, A. Bobrovsky, J. Stumpe, V. Shibaev, *Adv. Opt. Mater.* **2015**, *3*, 1273.

[33] A. Ryabchun, A. Sobolewska, A. Bobrovsky, V. Shibaev, J. Stumpe, *J. Polym. Sci., Part B: Polym. Phys.* **2014**, *52*, 773.

[34] L. M. Blinov, M. V. Kozlovsky, G. Cipparrone, *Chem. Phys.* **1999**, *245*, 473.

[35] H. C. Yeh, G. H. Chen, C. R. Lee, T. S. Mo, *Appl. Phys. Lett.* **2007**, *90*, 261103.

[36] P. Zhou, Y. Li, X. Li, S. Liu, Y. Su, *Liq. Cryst. Rev.* **2016**, *4*, 83.

[37] A. Shishido, *Polym. J.* **2010**, *42*, 525.

[38] F. K. Bruder, R. Hagen, T. Roelle, M. S. Weiser, T. Fäcke, *Angew. Chem., Int. Ed.* **2011**, *50*, 4552.

[39] S. Yoneyama, T. Yamamoto, O. Tsutsumi, A. Kanazawa, T. Shiono, T. Ikeda, *Macromolecules* **2002**, *35*, 8751.

[40] M. Häckel, L. Kador, D. Kropp, H. W. Schmidt, *Adv. Mater.* **2007**, *19*, 227.

[41] A. Saishoji, D. Sato, A. Shishido, T. Ikeda, *Langmuir* **2007**, *23*, 320.

[42] A. Natansohn, P. Rochon, *Adv. Mater.* **1999**, *11*, 1387.

[43] N. Viswanathan, D. Kim, S. Tripathy, *J. Mater. Chem.* **1999**, *9*, 1941.

[44] Y. Harada, K. Sakajiri, H. Kuwahara, S. Kang, J. Watanabe, M. Tokita, *J. Mater. Chem. C* **2015**, *3*, 3790.

[45] A. Bobrovsky, A. Ryabchun, A. Medvedev, V. Shibaev, *J. Photochem. Photobiol., A* **2009**, *206*, 46.

[46] A. Bogdanov, A. Bobrovsky, A. Ryabchun, A. Vorobiev, *Phys. Rev. E* **2012**, *85*, 011704.

[47] L. M. Goldenberg, V. Lisinetskii, A. Ryabchun, A. Bobrovsky, S. Schrader, *ACS Photonics* **2014**, *1*, 885.

[48] K. Urayama, Y. Okuno, T. Kawamura, S. Kohjiya, *Macromolecules* **2002**, *35*, 4567.

[49] F. Zhao, C. Wang, M. Qin, P. Zeng, P. Cai, *Opt. Commun.* **2015**, *338*, 461.

[50] S. R. Nersisyan, N. V. Tabiryan, L. Hoke, D. M. Steeves, *Opt. Express* **2009**, *17*, 1817.

[51] H. Ono, A. Emoto, F. Takahashi, N. Kawatsuki, T. Hasegawa, *J. Appl. Phys.* **2003**, *94*, 1298.

[52] H. J. Eichler, S. Orlic, R. Schulz, J. Rübner, *Opt. Lett.* **2001**, *26*, 581.

[53] L. Nikolova, T. Todorov, V. Dragostinova, T. Petrova, N. Tomova, *Opt. Lett.* **2002**, *27*, 92.

[54] D. K. Hore, A. L. Natansohn, P. L. Rochon, *J. Phys. Chem. B* **2003**, *107*, 2506.

[55] G. Cipparrone, P. Pagliusi, C. Provenzano, V. P. Shibaev, *Macromolecules* **2008**, *41*, 5992.

[56] R. M. Tejedor, J. L. Serrano, L. Oriol, *Eur. Polym. J.* **2009**, *45*, 2564.

[57] R. Arppe, T. J. Sørensen, *Nat. Rev. Chem.* **2017**, *1*, 0031.

[58] B. Javidi, A. Carnicer, M. Yamaguchi, T. Nomura, E. Pérez-Cabré, M. S. Millán, N. K. Nishchal, R. Torroba, J. F. Barrera, W. He, X. Peng, A. Stern, Y. Rivenson, A. Alfalou, C. Brosseau, C. Guo, J. T. Sheridan, G. Situ, M. Naruse, T. Matsumoto, I. Juvells, E. Tajahuerce, J. Lancis, W. Chen, X. Chen, P. W. H. Pinkse, A. P. Mosk, A. Markman, *J. Opt.* **2016**, *18*, 083001.

[59] Y. Geng, J. Noh, I. Drevensek-Olenik, R. Rupp, G. Lenzini, J. P. Lagerwall, *Sci. Rep.* **2016**, *6*, 26840.

[60] R. Balamurugan, J. H. Liu, *React. Funct. Polym.* **2016**, *105*, 9.

[61] C. C. Chien, J. H. Liu, A. V. Emelyanenko, *J. Mater. Chem.* **2012**, *22*, 22446.

[62] M. Portugall, H. Ringsdorf, R. Zentel, *Macromol. Chem. Phys.* **1982**, *183*, 2311.